DFT benchmark study of the O–O bond dissociation energy in peroxides validated with high-level *ab initio* calculations.

Danilo J. Carmona · **Pablo Jaque** ·
Esteban Vöhringer-Martinez

Abstract Peroxides play a central role in many chemical and biological processes such as the Fenton reaction. The relevance of these compounds lies in the low stability of the O–O bond which upon dissociation results in radical species able to initiate various chemical or biological processes. In this work, a set of 64 DFT functional-basis set combinations has been validated in terms of their capability to describe bond dissociation energies (BDE) for the O–O bond in a database of 14 $ROOH$ peroxides for which experimental values of BDE are available. Moreover, the electronic contributions to the BDE were obtained for four of the peroxides and the anion $H_2O_2^-$ at the CBS limit at CCSD(T) level with Dunning's basis sets up to triple–ζ quality providing a reference value for the hydrogen peroxide anion as a model. Almost all the functionals considered here yielded mean absolute deviations around $5.0\,\mathrm{kcal\,mol^{-1}}$. The smallest values were observed for the ωB97 family and the Minnesota M11 functional with a marked basis set dependence. Despite the mean deviation, order relations among BDE experimental values of peroxides were also considered. The ωB97 family was able to reproduce the relations correctly whereas other functionals presented a marked dependence on the chemical nature of the R group. Interestingly, M11 functional did not show a very good agreement with the established order despite its good performance in the mean error. The obtained results support the use of similar validation strategies for proper prediction of BDE or other molecular properties by DFT methods in subsequent related studies.

Keywords *ab initio* · Peroxides · DFT benchmark · CBS limit · BDE

Danilo J. Carmona and Esteban Vöhringer-Martinez
Departamento de Físico-Química, Facultad de Ciencias Químicas, Universidad de Concepción, Concepción, Chile. dacarmona@udec.cl, evohringer@udec.cl

Pablo Jaque
Departamento de Química Orgánica y Fisicoquímica, Facultad de Ciencias Químicas y Farmacéuticas, Universidad de Chile. Sergio Livingstone 1007, Independecia, Santiago, Chile. pablo.jaque@ciq.uchile.cl

1 Introduction

Peroxides are compounds with the general formula $ROOR'$, where R and R' correspond to any (generally organic) chemical group bonded through a covalent bond. These are naturally ubiquitous in the environment mainly because of atmospheric O_2, which can react, for instance, with water to form hydrogen peroxide (H_2O_2) [1]. In biological systems, H_2O_2 is widely known as a side product of the cellular reduction of O_2, which is coupled to the oxidation of nutrients [2–4]. In presence of reduced metallic cations as Fe^{2+}, the oxygen–oxygen bond cleavage in hydrogen peroxide is facilitated by the so called Fenton reaction [5, 6], where the subsequent formation of the strong oxidizing hydroxyl radical ($\cdot OH$) results in the destruction of cellular components as lipids, proteins and nucleic acids, leading to inflammatory processes, carcinogenesis and aging [7–10]. Peroxides have also been used in a wide range of industrial processes as the synthesis of polymeric resins [11, 12] and the removal of organic contaminants from water bodies [13, 14].

The biological and industrial role of peroxides is directly related to the low stability of the O–O bond in comparison with other compounds in which oxygen is bonded to elements of the second period [1]. Keeping this in mind, the theoretical characterization of the chemistry of peroxides should include a comprehensive study of the homolytic peroxide bond breaking (PBB). In our previous work, we performed a systematic study defining numerical descriptors associated to the PBB process in hydrogen peroxide and carrying out a benchmark study of the performance of DFT methods [15, 16] (64 functional–basis set combinations; Table 1) [17]. We first considered the bond dissociation energy (BDE) as an energetic descriptor, which is defined in the following way for a $ROOH$ peroxide:

$$BDE = \Delta_f H^0_{298.15}(RO\cdot) + \Delta_f H^0_{298.15}(\cdot OH) - \Delta_f H^0_{298.15}(ROOH) \quad (1)$$

A validation based on the BDE takes advantage of the availability of experimental reference data [18]. However, it is not easy to identify sources of error in its calculation from first principles because deviation from experimental data could be originated from the electronic structure and frequency calculations as well as from the inability of computational methods to describe other experimental conditions such as deviations from the ideal behavior. As an alternative, extrapolated CCSD calculations at the complete basis set (CBS) limit provide additional benchmark reference data reflected in the electronic energy (including internuclear repulsion) associated to the PBB process (electronic BDE, $eBDE$), which is defined as:

$$eBDE = E(RO\cdot) + E(\cdot OH) - E(ROOH) \quad (2)$$

In our recent study we observed good agreement of the BDE value of hydrogen peroxide calculated with several DFT–based methods compared to its experimental reference value of $50.35\,\mathrm{kcal\,mol^{-1}}$ [18]. The unsigned errors did not exceed $5.0\,\mathrm{kcal\,mol^{-1}}$ for almost all the tested functional–basis set combinations (Table 1). A basis set dependence explained in terms of qualitative arguments based on the features of each functional–basis set combination was also observed. Same trend was verified for the calculation of $eBDE$, whose reference value was obtained by performing highly correlated *ab initio* calculations. These results enabled us to conclude that the main source of error in the prediction of BDE is mainly dominated by the electronic structure description. The importance of a correct description of the electron correlation energy was evidenced from high level *ab initio* calculations and supported the feasibility of using DFT methods to computationally describe the PBB process in hydrogen peroxide [17].

Here, we study whether the conclusions for hydrogen peroxide can be extended to a total of 14 peroxides with the general formula $ROOH$, where the R group ranges from alkyl and alkoxy groups to halogen atoms. Criteria for the choice of $ROOH$ peroxides considered their chemical variability in terms of the number of atoms and elements present in the R group, the availability of experimental reference values for BDE and the feasibility of the calculation of a reference for $eBDE$. Their structure is shown in Table 2 together with a syntax used to differentiate them and their BDE experimental references. The hydrogen peroxide radical anion $H_2O_2^-$ was also included as a model system for the reaction in presence of metals as in the Fenton reaction, where the metallic center acts as a reducing agent transferring an electron to the peroxide bond [19].

For applications, choice of a peroxide within a group of candidates is often required instead of the knowledge of specific features of only one of them [6]. Therefore, rather than focusing only on the reproduction of the exact value of BDE we also analyzed whether the different functional–basis set combinations are able to reproduce BDE's trend among peroxides accounting for the experimental error.

Table 1: Chosen $E_{xc}[\rho]$ functionals and their features (UE and MUE values in $\mathrm{kcal\,mol^{-1}}$)

E_{xc} functional	MUE for BDE[a]	UE for BDE[b]	UE for eBDE[b]	Jacob's ladder rung	%HF [c]	RS function	Empirical fit	Ref.
N12	5.63	3.22	2.97	GGA	0	NO	YES	[20]
BLYP	11.66	2.26	1.60	GGA	0	NO	YES	[21, 22]
PBE	6.14	7.85	7.30	GGA	0	NO	NO	[23]
MN12L	4.85	3.40	3.47	mGGA	0	NO	YES	[24]
M06-L	7.75	4.21	4.53	mGGA	0	NO	YES	[25]
B3LYP	9.84	4.14	4.44	HGGA	20	NO	YES	[21, 22, 26]
PBE0	7.12	2.94	3.08	HGGA	25	NO	NO	[27]
SOGGA11-X	4.97	4.44	4.43	HGGA	40	NO	YES	[28]
ωB97	3.85	1.36	1.43	HGGA	0 - 100[d]	YES	YES	[29]
ωB97-X	4.45	1.82	1.89	HGGA	15 - 100[d]	YES	YES	[29]
ωB97-XD	4.52	1.84	1.93	HGGA	22 - 100[d]	YES	YES	[30]
BMK	3.78	2.99	3.05	HmGGA	42	NO	YES	[31]
M06	4.10	1.94	2.11	HmGGA	27	NO	YES	[25]
M06-2X	2.50	0.81	0.87	HmGGA	54	NO	YES	[25]
M05-2X	2.64	3.32	3.40	HmGGA	56	NO	YES	[32]
M11	3.13	0.12	0.26	HmGGA	43 - 100[d]	YES	YES	[33]

[a] Mean unsigned error for the $ABDE$12 database of Truhlar and Peverati (2014) [34]. [b] Unsigned error with regard to the experimental reference value of BDE or the electronic BDE reference ($eBDE$) obtained from extrapolated high level *ab-initio* calculations at the CBS limit for hydrogen peroxide [17]. MG3S basis set was used in both cases. [c] Percentage of Hartree–Fock exchange in hybrid functionals and [d] short and long range %HF for range–separated (RS) hybrid functionals. Note that in Minnesota–type MX and NX functionals incorporate the exchange and correlation terms in a separable and non–separable way, respectively.

Table 2: Chosen peroxides, their experimental reference values of BDE [18], syntax of the labels used in this manuscript for their R group and their corresponding ball–and–sticks models (obtained by using the software *Chemcraft* [35]).
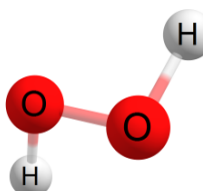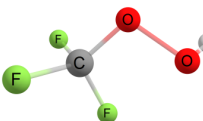
Peroxide	BDE/kcal mol^{-1}	Label	Structure
Hydroperoxy radical	65.55 ± 0.08	*rad*	
Hydrogen peroxide	50.35 ± 0.10	*H*	
Trifluoromethyl hydroperoxide	48.1 ± 5	CF_3	

Table 2: Chosen peroxides and their features (*Continued*)
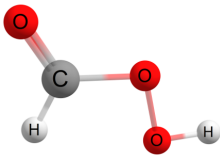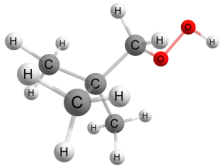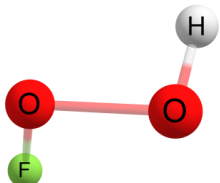
Peroxide	BDE/kcal mol^{-1}	Key	Structure
Zeroane	47.6 ± 2	CHO	
1-hydroperoxy-2,2-dimethylpropane	46.3 ± 1.9	$CH_2C(Me)_3$	
Fluoride hydroperoxide	45.6 ± 2	F	

Table 2: Chosen peroxides and their features (*Continued*)
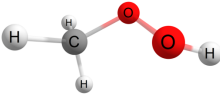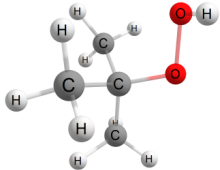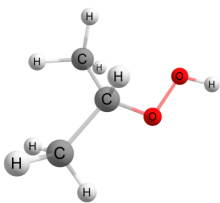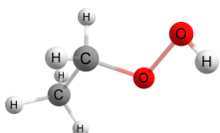
Peroxide	BDE/kcal mol^{-1}	Key	Structure
Methyl hydroperoxide	45.2 ± 1	*Me*	
Tert-butyl hydroperoxide	44.8 ± 0.5	$t-but$	
Isopropyl hydroperoxide	44.4 ± 1.5	*isopropyl*	
Ethyl hydroperoxide	42.7 ± 1.5	*Et*	

Table 2: Chosen peroxides and their features (*Continued*)
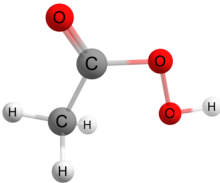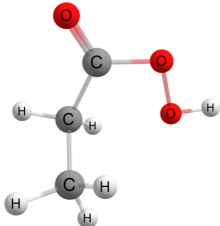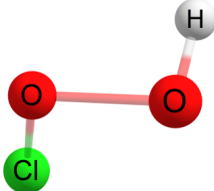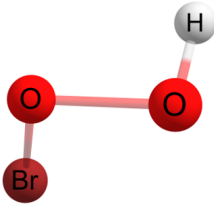
Peroxide	BDE/kcal mol^{-1}	Key	Structure
Methaneperoxycarboxylic Acid	40.6 ± 0.5	*CMeO*	
Ethaneperoxycarboxylic Acid	40.6 ± 0.5	*CEtO*	

Table 2: Chosen peroxides and their features (*Continued*)

Peroxide	BDE/kcal mol^{-1}	Key	Structure
Cloroperoxide	35	*Cl*	
Bromo hydroxide	33.1 ± 2	*Br*	

2 Methods

All peroxides listed in Table 2 together with hydrogen peroxide anion ($H_2O_2^-$) were considered in this work. Reference values for $eBDE$ were obtained using highly correlated *ab initio* calculations for the peroxides containing the R groups H (reference peroxide), Cl (electron-withdrawing group), Et and $CMeO$ (bulky aliphatic and electron withdrawing group). Calculations were carried out considering Unrestricted Hartree–Fock determinants (UHF) at the CCSD(T) level using the complete basis set (CBS) extrapolation scheme of Halkier et al. [36] combined with Dunning's basis sets [37–39] up to triple–ζ quality. Geometries optimized at B3LYP/6-31+G(d,p) level of theory were used for the four $ROOH$ peroxides (for a justification, see section S.1 in supporting information). All these calculations were performed using the PSI 4 program [40] coupled to the MRCC suite [41].

Assessment of DFT–based methods was performed in the same way as in our previous work [17]: geometry optimization and frequency calculations of $ROOH$ peroxides, $\cdot OR$ and $\cdot OH$ radicals were carried out in order to confirm minimum energy structures on the potential energy surfaces (zero imaginary frequencies) and to obtain formation enthalpies of these species. BDE and $eBDE$ values (Equations 1 and 2) were calculated for each functional–basis set combination from the obtained structures. All electron condition and the command $grid = ultrafine$ for the numerical computation of integrals were considered in all the calculations, carried out using the *Gaussian 09* package of programs [42].

Exchange–correlation functionals (E_{xc}) used in the calculation of $eBDE$ and BDE values and their main features are shown in Table 1. This choice is the same as in our previous work [17]; these are covering a wide range in the so called Jacob's ladder and reproducing BDE values in the database $ABDE12$ used by Peverati and Truhlar in 2014 [34]. Moreover, inclusion of range separated hybrid functionals and empirical parameters in the design of functionals were also selection criteria.

The effect of the basis set was tested by comparing four Pople's basis sets, which may determine the flexibility of the electron density (i.e. its homogeneity vs. non–homogeneity) as previously described by us [17]: MG3S basis set (6-311+G(2df,2p)) [43] was the starting point because this was used in the databases of Peverati and Truhlar in 2014 [34]. To reduce the computational cost the 6-31G(d,p) basis set was considered and then by successively adding diffuse functions and splitting the valence one arrives to the 6-31+G(d,p) and 6-311+G(d,p) basis sets, respectively. The MG3S basis set is obtained by adding polarization functions to the lastly considered set. Only basis sets including diffuse functions were considered to ensure a correct description of the hydroxyl anion [44].

For a particular $ROOH$ peroxide, performance of each functional–basis set combination was firstly given by the computation of signed and unsigned error (SE and UE, respectively):

$$SE = \text{Calculated value} - \text{Reference value} \qquad UE = |SE| \qquad (3)$$

Mean signed and unsigned errors (MSE and MUE, respectively) were also computed as stated in equation 4:

$$MSE = \frac{\sum_{\text{peroxides}} SE}{n_{\text{peroxides}}} \qquad\qquad MUE = \frac{\sum_{\text{peroxides}} UE}{n_{\text{peroxides}}} \qquad (4)$$

Statement of an order relation among the experimental reference BDE values of the peroxides in Table 2 was made by considering their general form:

$$BDE(X) = \overline{BDE(X)} \pm err(X) \qquad (5)$$

where $\overline{BDE(X)}$ and $err(X)$ correspond respectively to the average experimental value and its associated error for an arbitrary $ROOH$ peroxide X. Considering the value of $1.0\,\text{kcal}\,\text{mol}^{-1}$ as a suitable bound of chemical accuracy, the following order relation on the set of the experimental reference values of BDE is defined in this work:

$$\begin{aligned} BDE(B) > BDE(A) \Leftrightarrow \\ \left[\overline{BDE(B)} - err(B) - 1.0\,\text{kcal}\,\text{mol}^{-1}\right] > \\ \left[\overline{BDE(A)} + err(A) + 1.0\,\text{kcal}\,\text{mol}^{-1}\right] \end{aligned} \qquad (6)$$

From equation 6, the useful parameter Δ can be defined, where the relation $\overline{BDE(B)} > \overline{BDE(A)}$ is kept:

$$\Delta = \left[\overline{BDE(B)} - err(B)\right] - \left[\overline{BDE(A)} + err(A)\right] \qquad (7)$$

and therefore:

$$\begin{aligned} BDE(B) > BDE(A) \Leftrightarrow \\ \Delta > 2.0\,\text{kcal}\,\text{mol}^{-1} \end{aligned} \qquad (8)$$

With this order relation diagram in Figure 2a summarizes all possible order relations among the experimental BDE reference values. For the validation of DFT methods from this point of view, any wrongly reproduced order relation is defined as a "penalty" and the total number of penalties per DFT–based method was used as an additional performance criterion.

3 Results and discussion

To exclude that deviations from experimental BDE reference values are due
to factors different from the correct description of the electronic structure of
the involved species, the calculation of $eBDE$ was considered. As reference
we took CCSD(T) calculations extrapolated to the complete basis set (CBS)
limit as described in the Methods section. This analysis encompassed only five
peroxides: H, Et, Cl, $CMeO$ and the anion of hydrogen peroxide ($H_2O_2^-$)
due to the computational cost. The geometries for these calculations were ob-
tained at the B3LYP/6-31+G(d,p) level because this combination presented
a deviation of only $0.01\,\mathrm{kcal\,mol^{-1}}$ in the $eBDE$ value of hydrogen perox-
ide in comparison with that calculated with the experimental geometry (see
section S.1 in Supporting Information). For the neutral species H, Et, Cl
and $CMeO$, our results show the same trend for $eBDE$ as in BDE calcula-
tions (see sections S.2, S.3 and S.4 in Supporting Information). These facts
lead us to establish a necessary condition to ensure that different performance
among methods arises from the electronic structure part of the calculation as
previously observed for the hydrogen peroxide [17]. Moreover, this supports
that CCSD(T)/CBS calculations in combination with DFT geometries and
thermal corrections are able to predict the experimental BDE values within
chemical accuracy at least for these neutral peroxides (Table 3). In the case of
the anion of hydrogen peroxide ($H_2O_2^-$) a reference $eBDE$ of $7.75\,\mathrm{kcal\,mol^{-1}}$
was obtained. As it was expected, this value is smaller compared to the other
peroxides by at least $20.0\,\mathrm{kcal\,mol^{-1}}$, although ZPE and thermal contribu-
tion is practically constant among methods, which allowed us to anticipate
a BDE reference value for the anion (Table 3). However, $eBDE$ calculated
using DFT methods for this species deviates by at least $20.0\,\mathrm{kcal\,mol^{-1}}$ from
the $ab\ initio$ reference. Additionally, these methods did not always predict a
smaller $eBDE$ value for $H_2O_2^-$ compared to the neutral peroxides (see section
S.5 in the Supporting Information). Wrong description of parameters includ-
ing anionic species had just been described in our previous work [17], where a

Table 3: $ab\ initio\ eBDE$ and predicted BDE values for
the selected set of five peroxides. All values in $\mathrm{kcal\,mol^{-1}}$.

Peroxide	eBDE[a]	TZC[b]	$\mathbf{BDE}_{pred}$[c]	$\mathbf{BDE}_{exp}$[d]
H_2O_2	55.17	-4.48	50.69	50.35 ± 0.1
$Me(CO)OOH$	45.95	-3.92	42.03	40.6 ± 0.5
$ClOOH$	38.13	-2.83	35.30	35 ± 5
$EtOOH$	50.18	-5.11	45.07	42.7 ± 1.5
$H_2O_2^-$	7.75	-1.21	6.54	-

[a] Calculated as described in section 2; [b] Thermal and ZPE con-
tribution calculated at B3LYP/6-31+G(d,p) level; [c] $BDE_{pred} =
eBDE + TZC$; [d] See Luo et al. [18].

non systematic trend was obtained for the electron affinity of hydroxyl radical by using the same set of functional–basis set combinations considered here.

Having found enough evidence for the feasibility of explaining differences among *DFT* methods in the reproduction of *BDE* values through arguments based on the electronic structure of the systems, we performed our further analysis based on deviations from experimental *BDE* reference data. Figure 1a summarizes the mean unsigned error (MUE) and mean signed error (MSE) for bond dissociation energies (*BDE*) calculated for the peroxide database with different functionals and basis sets compared to the results of hydrogen peroxide reported recently by us (Figure 1b) [17]. For hydrogen peroxide we established that the signed error (see inset) decreases for all functionals when the basis set is augmented from 6-31G(d,p) to 6-31+G(d,p) and 6-311+G(d,p) but increases with the inclusion of polarization functions (MG3S basis set [43]). This trend is confirmed for all peroxides as the insets of SE on Figures 1a and S.1 (supporting information) reveal. The inclusion of diffuse functions and more functions for the valence shells leads to smaller *BDE* values because of the electronic energy of the radicals $\cdot OH$ and $\cdot OR$ becomes more negative faster compared to the peroxides *ROOH* when the basis set is enhanced, probably due to the increased flexibility of the larger basis sets, i.e. the so-called size–extensivity problem. The opposite is observed when passing from 6-311+G(d,p) to 6-311+G(2df,2p) (MG3S) because the addition of polarization functions implies the inclusion of d and f atomic orbitals, which generates a displacement of the electronic density of a nature different from such observed for the addition of s and p atomic orbitals. Therefore, it is not surprising that the behavior of density functionals changes when these modifications on the basis set are made, specifically in terms of the energy variation of the reactant *ROOH* in comparison with such observed for the products $\cdot OH$ and $\cdot OR$ (see insets on Figure 1 and Figure S.1 in supporting information).

For GGA functionals (N12, BLYP and PBE) all SE were positive for hydrogen peroxide but this trend is not confirmed for all peroxides. Comparing the SE of the different peroxides two groups are distinguished: peroxides with R consisting of less than two atoms ($R = H$,Cl, F, rad and Br) present the same behavior as hydrogen peroxide, and the other ones, where the R group consists of more than one atom, present negative SE for these three functionals (see Figure S.1 in Supporting Information). The SE is most negative for R–groups containing an oxygen atom as the ketones. The dissimilar behavior of these two groups of peroxides explains the small values of MSE when the SEs are averaged over all peroxides. For the remaining functionals (meta–GGA and hybrids), the behavior is approximately uniform among peroxides.

One has to consider that the approximate form of E_{xc} functionals is often parameterized on energy differences rather than on the absolute electronic energy. Therefore, the unsigned error is more appropriate to assess their performance for peroxides. For GGA functionals, basis set dependence observed

for UE in $HO - OH$ (Figure 1b) is attenuated when MUE values are calculated (Figure 1a). This fact is a numerical consequence that the basis set dependence on UE for peroxides with positive SE values is inverse to the other ones (for example, compare CH_2CMe_3 and F in Figures S.1d and S.1e in supporting information). This is ultimately originated by the just commented basis set dependence on SE, which is present in all the here considered peroxides, as pointed in the second paragraph of this section. Non–local functionals (meta–GGA and hybrid ones) present a basis set dependence where the MUE increases in the order 6-31G(d,p) to 6-31+G(d,p) and 6-311+G(d,p) and decreases for MG3S in accordance with the result of hydrogen peroxide. This is a direct consequence that these functionals do not present the dependence on the R group as observed for GGA functionals. This could indicate that inclusion of certain amount of exact non–local HF exchange improves the agreement with reference values for the peroxides with larger R group consisting of more than one atom. Non–local range separated functionals as the ωB97 family and M11 show smaller MUE, specifically for the combination M11/MG3S, which has just been reported by us as a good method for hydrogen peroxide [17]. The only functional including dispersion effects on this set is ωB97X-D, whose good performance can not be attributed exclusively to this feature, since this is not the only difference with other functionals, even in the case of ωB97X, because the correlation term was also reparameterized [30]. To support even more this argument, we assayed the effect of including dispersion by calculating eBDE values for the small reference peroxide $HO - OH$ with the small basis set 6-31+G(d,p) and for the large peroxide CH_2CMe_3 with the largest basis set used here (MG3S). We performed these calculations using the functional B3LYP including the D3 dispersion correction. Differences with regard to the B3LYP functional ranged only from $0.25\,\mathrm{kcal\,mol^{-1}}$ (for $HO - OH$) to $1.00\,\mathrm{kcal\,mol^{-1}}$ for CH_2CMe_3. Yet, in general the MUE of all peroxides are larger than the values for hydrogen peroxide probably because of the dependence of the error on the number of electrons in the system. This is mainly the case for peroxides with R groups consisting of more than one atom, for which the values of MUE can exceed 7.0 or even $10.0\,\mathrm{kcal\,mol^{-1}}$ for hybrid functionals as B3LYP or PBE0 (see Figure S.1 in Supporting Information). Because of its dependence on the cardinality of the basis set and therefore on the number of electrons, we also computed BSSE corrections for the small reference peroxide $HO - OH$ with the small basis set 6-31+G(d,p), and for the large peroxide CH_2CMe_3 with the largest basis set used here (MG3S). These calculations were performed with the robust functional B3LYP. Difference in BSSE was only $0.11\,\mathrm{kcal\,mol^{-1}}$ ($1.00\,\mathrm{kcal\,mol^{-1}}$ for $HO - OH$ and $0.89\,\mathrm{kcal\,mol^{-1}}$ for CH_2CMe_3), which allow us to argue BSSE is not a quantity whose consideration affects the interpretation of the obtained results through the set of peroxides.

For some applications it is more important to establish an order relation among the BDE reference values of the different peroxides rather than the reproduction of absolute bond dissociation energies to anticipate which peroxide would
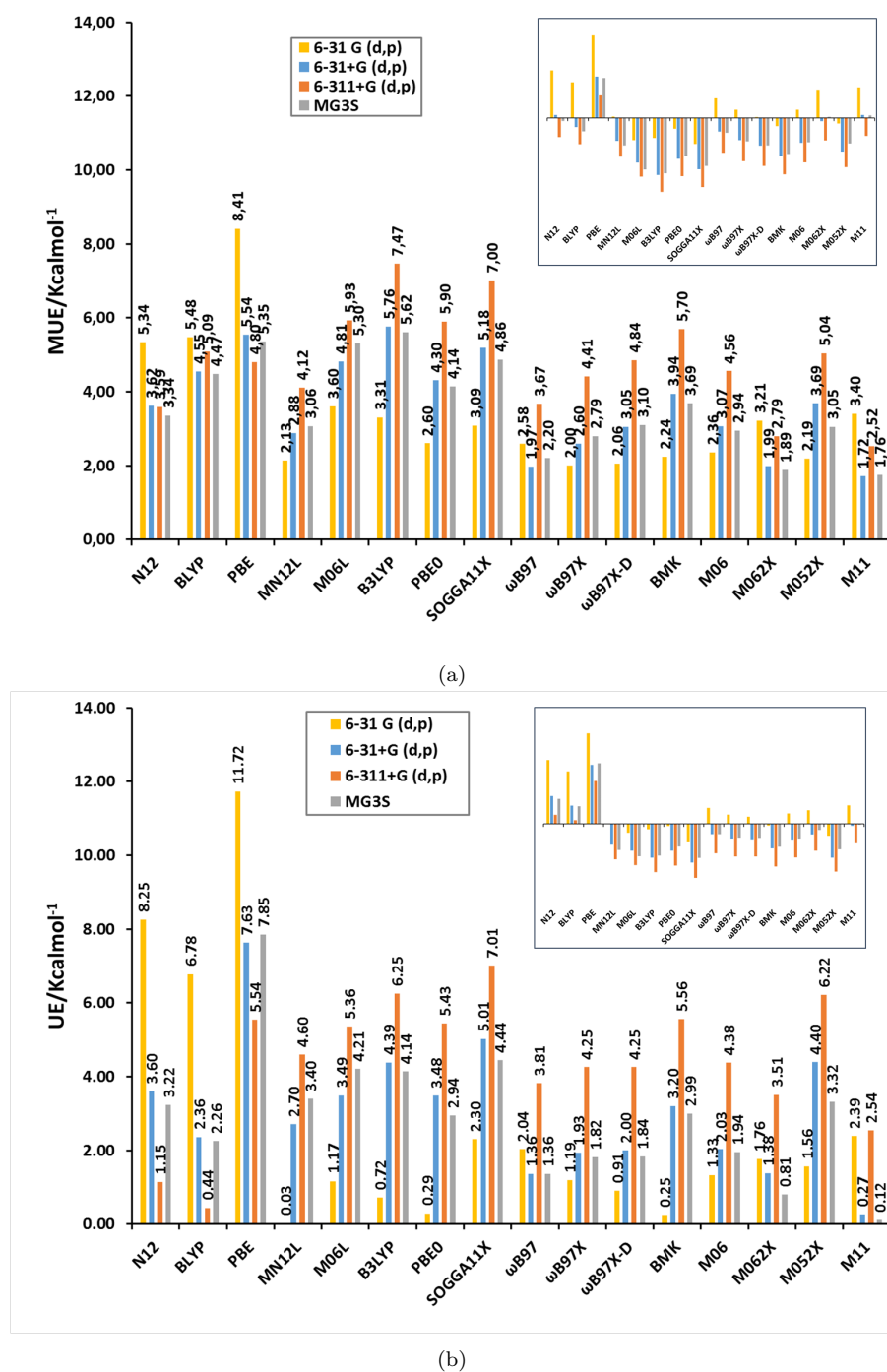
(a)

(b)

Figure 1: (a) Mean unsigned error (MUE) of the calculated values of BDE with different DFT methods for the peroxide database with regard to the experimental reference values. Inserted graph shows the corresponding mean Signed error (MSE) values. (b) Unsigned (UE) and signed error (SE) for hydrogen peroxide as comparison.

dissociate more easily. The reactivity order map shown in Figure 2a relates the experimental values and is used as reference to quantify what functional–basis set combination reproduces the experimental reactivity order. If a DFT method does not reproduce correctly one of the 50 order relations established in the Figure 2a, then a penalty is assigned. The overall number of penalties for the tested DFT methods are summarized in Figure 2b. The ωB97X-D [30] functional presents the lowest number of penalties besides the just described low value of MUE. However, the M11 Minnesota functional [33], which showed small values of MUE, presents a large number of penalties. This suggest that this functional might reduce MUE possibly due to the number of parameters it contains, but it is less robust in the reproduction of the BDE order among different peroxides. Therefore, if the order of BDE is of interest the ωB97 family of functionals seems to be more appropriate probably due to the inclusion of a range separation function, which is an effect not depending on the empirical fit that differentiate them from other similar functionals like B3LYP [29].

To further analyze the performance of DFT functionals, we show in Table 4 order relations for which at least one penalty was detected, their number of penalties and the associated Δ values. The fact that there is not a correlation between the Δ value and the amount of penalties allows us to conclude that the main source of penalties relies on the features of the functional–basis set combinations (Table 4). To study the chemical nature of the penalties we analyzed their distribution among different R groups. Table 4 shows that peroxides with R groups $CH_2C(Me)_3$ and $CMeO$ clearly possess larger number of penalties with regard to the total order relations in which they are involved (Figure 3). This fact could be derived from the larger fluctuations in the computed BDE values for these species as discussed before for the MSE, mainly in the case of GGA functionals.
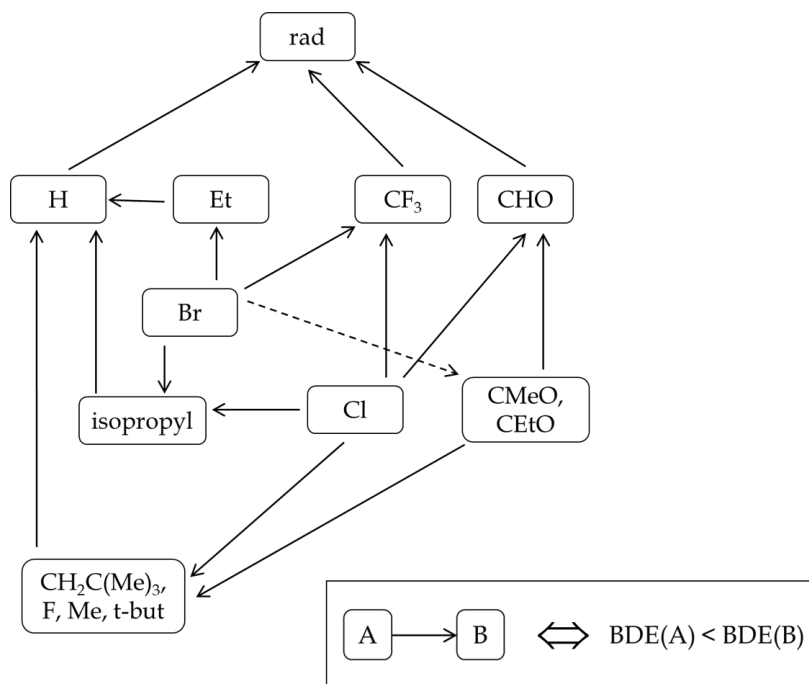
(a)
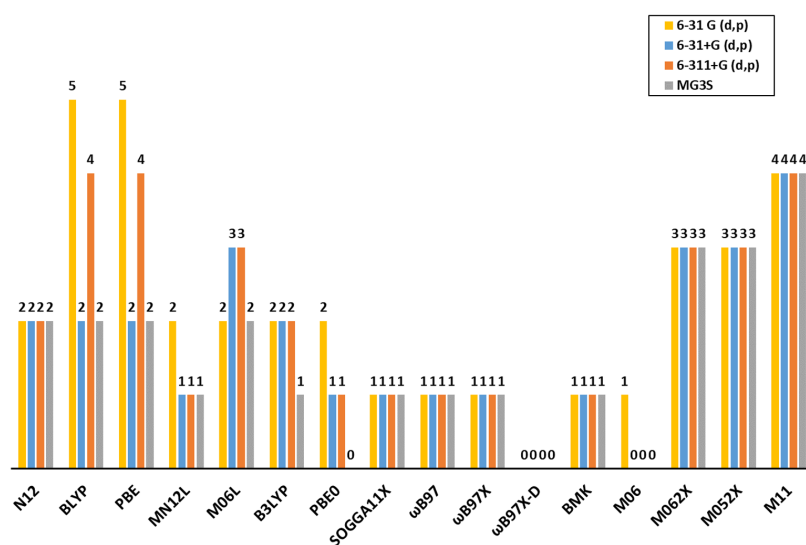
(b)

Figure 2: (a) Map showing the order relations among the experimental reference BDE values for the peroxides considered in this study. Arrows point to peroxide with higher BDE value, as indicated in the inset. (b) Penalties committed by each DFT method in the reproduction of the 50 order relations shown in the map of part (a).

Table 4: BDE order relations for which penalties were commited by the DFT methods considered here.

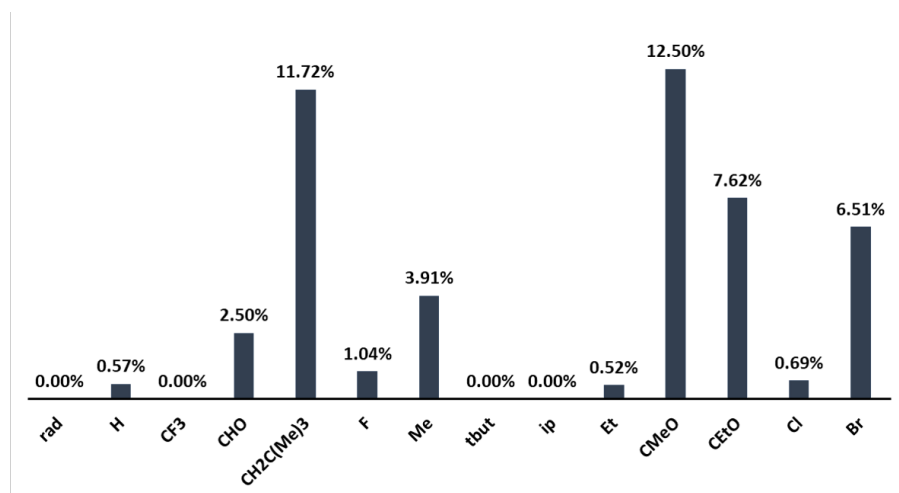| Order relation	Penalties	$\Delta/\ kcal\ mol^{-1}$
CMeO → CH$_2$C(Me)$_3$	32	3.3
Br → CEtO	25	5.0
Br → CMeO	19	5.0
CMeO → Me	12	3.1
CEtO → CH$_2$C(Me)$_3$	11	3.3
Cl → CHO	4	5.6
Br → CHO	4	10.5
F → H	3	2.65
CEtO → Me	3	3.1
Br → CH$_2$C(Me)$_3$	2	9.3
Et → H	1	6.05
CMeO → F	1	2.5

Figure 3: Percentage of penalties committed by all considered DFT methods for peroxides with different R groups.

4 Conclusions

In this work, we have extended our previous validation of 64 systematically chosen DFT functional–basis set combinations in the description of BDE and $eBDE$ values for the hydrogen peroxide [17] to a set of 14 $ROOH$ peroxides for which experimental data of BDE are available. In general terms, error trends observed in hydrogen peroxide are conserved in the case of non–local functionals (meta–GGA and hybrid ones): same basis set dependence is verified for each functional in the reproduction of $eBDE$ and BDE, which suggests that variation among results mainly arises from the electronic structure part of the calculation. This fact allows us to give an explanation of these differences through arguments based on the electronic structure and at the same time to make a rational choice of the functional–basis set combination when computational calculations of BDE or $eBDE$ are required. Within these non–local functionals the $\omega B97$ family present smaller absolute deviations for all the peroxides. Local GGA functionals show a specie–depending behavior that can be rationalized in terms of the amount of atoms and elements present in the R group. Therefore, this validation does not only constitute a report of error values but it also provides a rational strategy for the choice of functional–basis sets based on the features of the functional, the basis set and the specific peroxide to be described.

The performance was not only based on the calculation of deviations from reference values but it considered the establishment of a reactivity order to evaluate the extent on which DFT methods are capable to reproduce it. Although in general all the DFT methods reproduced the order relations in at least a 90%, this analysis evidenced some differences between the $\omega B97$ family and M11 functionals, which both present the smallest absolute deviation from the reference values. Yet, the order is only well reproduced by the first one. We conclude that the establishment of a reactivity order is a valuable strategy for a subsequent validation of DFT methods, for example, in applications where the choice of a certain material is required instead of predicting a specific value. The outcome of this validation enables us to recommend DFT for the study of bond dissociation energy order among peroxides.

Finally, we have also obtained a reference value for the anion $H_2O_2^-$ from first principles. This value could serve as a powerful reference to study the dissociation process considering this anion as a limit case of the peroxide bond breaking as a consequence of the reduction of the hydrogen peroxide, for example, by metallic centers as in the Fenton reaction [19]. However, this work also emphasizes caution in the use of DFT methods when anionic systems are intended to be described, as we have noted in our previous work for the electron affinity of hydroxyl radical [17].

Acknowledgements

References

1. Zvi Rappoport. *The chemistry of peroxides*. John Wiley & Sons, Chichester, 2006.
2. Dmitry B. Zorov, Magdalena Juhaszova, and Steven J. Sollott. Mitochondrial reactive oxygen species (ROS) and ROS-induced ROS release. *Physiological Reviews*, 94(3):909–950, 2014. PMID: 24987008.
3. Alejandro Romero, Eva Ramos, Cristobal de Los Rios, Javier Egea, Javier del Pino, and Russel J. Reiter. A review of metal-catalyzed molecular damage: protection by melatonin. *Journal of Pineal Research*, 56(4):343–370, 2014.
4. Sandrine Pouvreau. Genetically encoded reactive oxygen species (ROS) and redox indicators. *Biotechnology Journal*, 9(2):282–293, 2014.
5. H. J. H. Fenton. LXXIII.-Oxidation of tartaric acid in presence of iron. *J. Chem. Soc., Trans.*, 65:899, 1894.
6. Alok D Bokare and Wonyong Choi. Review of iron-free Fenton-like systems for activating H_2O_2 in advanced oxidation processes. *J Hazard Mater*, 275:121, 2014.
7. Minmin Zhang and Chang-Hyun Jang. Imaging the oxidation effects of the Fenton reaction on phospholipids at the interface between aqueous phase and thermotropic liquid crystals. *Journal of bioscience and bioengineering*, 120(2):193–198, 2015.
8. Mark Rinnerthaler, Johannes Bischof, Maria Streubel, Andrea Trost, and Klaus Richter. Oxidative stress in aging human skin. *Biomolecules*, 5(2):545–589, 2015.
9. M Valko, H Morris, and M Cronin. Metals, toxicity and oxidative stress. *Current medicinal chemistry*, 12(10):1161–1208, 2005.
10. C Lehmann, S Islam, S Jarosch, J Zhou, D Hoskin, A Greenshields, N Al-Banna, N Sharawy, A Sczcesniak, and M Kelly. The utility of iron chelators in the management of inflammatory disorders. *Mediators of inflammation*, 2015, 2015.
11. Gerald O. Wilson, James W. Henderson, Mary M. Caruso, Benjamin J. Blaiszik, Patrick J. McIntire, Nancy R. Sottos, Scott R. White, and Jeffrey S. Moore. Evaluation of peroxide initiators for radical polymerization-based self-healing applications. *Journal of Polymer Science Part A: Polymer Chemistry*, 48(12):2698–2708, 2010.
12. Jimmie C. Oxley, Joseph Brady, Steven A. Wilson, and James L. Smith. The risk of mixing dilute hydrogen peroxide and acetone solutions. *Journal of Chemical Health and Safety*, 19(2):27 – 33, 2012.
13. Maryam Salimi, Ali Esrafili, Mitra Gholami, Ahmad Jonidi Jafari, Roshanak Rezaei Kalantary, Mahdi Farzadkia, Majid Kermani, and Hamid Reza Sobhi. Contaminants of emerging concern: a review of new approach in AOP technologies. *Environmental Monitoring and Assessment*, 189(8):414, Jul 2017.
14. Arjunan Babuponnusami and Karuppan Muthukumar. A review on Fenton and improvements to the Fenton process for wastewater treatment. *Journal of Environmental Chemical Engineering*, 2(1):557 – 572, 2014.
15. P. Hohenberg and W. Kohn. Inhomogeneous electron gas. *Phys. Rev.*, 136:B864, 1964.
16. W. Kohn and L. J. Sham. Self-consistent equations including exchange and correlation effects. *Phys. Rev.*, 140:A1133, 1965.
17. Danilo J Carmona, David R Contreras, Oscar A Douglas-Gallardo, Stefan Vogt-Geisse, Pablo Jaque, and Esteban Vöhringer-Martinez. A systematic electronic structure study of the O–O bond dissociation energy of hydrogen peroxide and the electron affinity of the hydroxyl radical. *Theoretical Chemistry Accounts*, 137(9):126, 2018.
18. Yu-Ran Luo. *Comprehensive handbook of chemical bond energies*. CRC press, 2007.
19. Bernd Ensing, Francesco Buda, and Evert Jan Baerends. Fenton-like chemistry in water: oxidation catalysis by Fe (III) and H_2O_2. *The Journal of Physical Chemistry A*, 107(30):5722–5731, 2003.
20. Roberto Peverati and Donald G Truhlar. Exchange–correlation functional with good accuracy for both structural and energetic properties while depending only on the density and its gradient. *J. Chem. Theory Comput*, 8(7):2310, 2012.
21. Axel D Becke. Density-functional exchange-energy approximation with correct asymptotic behavior. *Phys. rev. A*, 38(6):3098, 1988.
22. Chengteh Lee, Weitao Yang, and Robert G Parr. Development of the Colle-Salvetti correlation-energy formula into a functional of the electron density. *Phys. rev. B*, 37(2):785, 1988.

23. John P Perdew, Kieron Burke, and Matthias Ernzerhof. Generalized gradient approximation made simple. *Phys. rev. lett*, 77(18):3865, 1996.
24. Roberto Peverati and Donald G Truhlar. An improved and broadly accurate local approximation to the exchange–correlation density functional: The MN12-L functional for electronic structure calculations in chemistry and physics. *Phys. Chem. Chem. Phys*, 14(38):13171, 2012.
25. Yan Zhao and Donald G Truhlar. The M06 suite of density functionals for main group thermochemistry, thermochemical kinetics, noncovalent interactions, excited states, and transition elements: two new functionals and systematic testing of four M06-class functionals and 12 other functionals. *Theor. Chem. Acc*, 120(1-3):215, 2008.
26. PJ Stephens, FJ Devlin, CFN Chabalowski, and Michael J Frisch. Ab initio calculation of vibrational absorption and circular dichroism spectra using density functional force fields. *J. Phys. Chem.*, 98(45):11623, 1994.
27. Carlo Adamo and Vincenzo Barone. Toward reliable density functional methods without adjustable parameters: The PBE0 model. *J. Chem. Phys*, 110(13):6158, 1999.
28. Roberto Peverati and Donald G Truhlar. Communication: A global hybrid generalized gradient approximation to the exchange-correlation functional that satisfies the second-order density-gradient constraint and has broad applicability in chemistry, 2011.
29. Jeng-Da Chai and Martin Head-Gordon. Systematic optimization of long-range corrected hybrid density functionals. *J. Chem. Phys*, 128(8):084106, 2008.
30. Jeng-Da Chai and Martin Head-Gordon. Long-range corrected hybrid density functionals with damped atom–atom dispersion corrections. *Phys. Chem. Chem. Phys*, 10(44):6615, 2008.
31. A Daniel Boese and Nicholas C Handy. A new parametrization of exchange–correlation generalized gradient approximation functionals. *J. Chem. Phys*, 114(13):5497, 2001.
32. Yan Zhao, Nathan E Schultz, and Donald G Truhlar. Design of density functionals by combining the method of constraint satisfaction with parametrization for thermochemistry, thermochemical kinetics, and noncovalent interactions. *J. Chem. Theory Comput*, 2(2):364, 2006.
33. Roberto Peverati and Donald G Truhlar. Improving the accuracy of hybrid meta-gga density functionals by range separation. *J. Phys. Chem. Lett*, 2(21):2810, 2011.
34. Roberto Peverati and Donald G Truhlar. Quest for a universal density functional: the accuracy of density functionals across a broad spectrum of databases in chemistry and physics. *Phil. Trans. R. Soc. A*, 372(2011):20120476, 2014.
35. Chemcraft - graphical software for visualization of quantum chemistry computations. https://www.chemcraftprog.com.
36. Asger Halkier, Trygve Helgaker, Poul Jorgensen, Wim Klopper, and Jeppe Olsen. Basis-set convergence of the energy in molecular Hartree–Fock calculations. *Chemical Physics Letters*, 302(5):437 – 446, 1999.
37. Thom H. Dunning. Gaussian basis sets for use in correlated molecular calculations. I. The atoms boron through neon and hydrogen. *The Journal of Chemical Physics*, 90(2):1007–1023, 1989.
38. David E. Woon and Thom H. Dunning. Gaussian basis sets for use in correlated molecular calculations. III. The atoms aluminum through argon. *The Journal of Chemical Physics*, 98(2):1358–1371, 1993.
39. David E. Woon and Thom H. Dunning. Gaussian basis sets for use in correlated molecular calculations. V. Core valence basis sets for boron through neon. *The Journal of Chemical Physics*, 103(11):4572–4585, 1995.
40. Robert M. Parrish, Lori A. Burns, Daniel G. A. Smith, Andrew C. Simmonett, A. Eugene DePrince, Edward G. Hohenstein, Uur Bozkaya, Alexander Yu. Sokolov, Roberto Di Remigio, Ryan M. Richard, Jrme F. Gonthier, Andrew M. James, Harley R. McAlexander, Ashutosh Kumar, Masaaki Saitow, Xiao Wang, Benjamin P. Pritchard, Prakash Verma, Henry F. Schaefer, Konrad Patkowski, Rollin A. King, Edward F. Valeev, Francesco A. Evangelista, Justin M. Turney, T. Daniel Crawford, and C. David Sherrill. Psi4 1.1: An open-source electronic structure program emphasizing automation, advanced libraries, and interoperability. *J. Chem. Theory Comput*, 13(7):3185, 2017.

41. M Kllay, Z Rolik, J Csontos, I Ladjanszki, L Szegedy, B Ladoczki, G Samu, K Petrov, M Farkas, and P Nagy. Mrcc, a quantum chemical program suite. *URL: http://www. mrcc. hu, accessed August 26th*, 2016.

42. M. J. Frisch, G. W. Trucks, H. B. Schlegel, G. E. Scuseria, M. A. Robb, J. R. Cheeseman, G. Scalmani, V. Barone, B. Mennucci, G. A. Petersson, H. Nakatsuji, M. Caricato, X. Li, H. P. Hratchian, A. F. Izmaylov, J. Bloino, G. Zheng, J. L. Sonnenberg, M. Hada, M. Ehara, K. Toyota, R. Fukuda, J. Hasegawa, M. Ishida, T. Nakajima, Y. Honda, O. Kitao, H. Nakai, T. Vreven, J. A. Montgomery, Jr., J. E. Peralta, F. Ogliaro, M. Bearpark, J. J. Heyd, E. Brothers, K. N. Kudin, V. N. Staroverov, R. Kobayashi, J. Normand, K. Raghavachari, A. Rendell, J. C. Burant, S. S. Iyengar, J. Tomasi, M. Cossi, N. Rega, J. M. Millam, M. Klene, J. E. Knox, J. B. Cross, V. Bakken, C. Adamo, J. Jaramillo, R. Gomperts, R. E. Stratmann, O. Yazyev, A. J. Austin, R. Cammi, C. Pomelli, J. W. Ochterski, R. L. Martin, K. Morokuma, V. G. Zakrzewski, G. A. Voth, P. Salvador, J. J. Dannenberg, S. Dapprich, A. D. Daniels, . Farkas, J. B. Foresman, J. V. Ortiz, J. Cioslowski, and D. J. Fox. Gaussian 09 Revision E.01. Gaussian Inc. Wallingford CT 2009.

43. Benjamin J Lynch, Yan Zhao, and Donald G Truhlar. Effectiveness of diffuse basis functions for calculating relative energies by density functional theory. *J. Phys. Chem. A*, 107(9):1384, 2003.

44. Timothy J Lee and Henry F Schaefer III. Systematic study of molecular anions within the self-consistent-field approximation: OH^-, CN^-, C_2H^-, NH_2^-, and CH_3^-. *J. Chem. Phys*, 83(4):1784, 1985.